High-Frequency Resonant Overvoltages in Transformer Regulating Winding Caused by Ground Fault Initiation on Feeding Cable

Bjørn Gustavsen, *Fellow*, *IEEE*, Alvaro Portillo, *Senior Member*, *IEEE*, Rodrigo Ronchi, *Member*, *IEEE*, and Asgeir Mjelve, *Member*, *IEEE*

***Abstract*—Transformer terminal equivalents obtained via admittance measurements are suitable for simulating high-frequency transient interaction between the transformer and the network. This paper augments the terminal equivalent approach with a measurement-based voltage transfer function model which permits calculation of voltages at internal points in the regulating winding. The approach is demonstrated for a single-phase three-winding transformer with its tap setting in the middle position. Three internal points in the regulating winding are included that represent the mid-point and the two extreme ends. The terminal equivalent modeling makes use of additional common-mode measurements to avoid error magnifications to result from the ungrounded tertiary winding. The final model is used in a time domain simulation where ground-fault initiation results in a resonant voltage build-up in the winding. It is shown that that the peak value of the resonant overvoltage can be higher than during the lightning impulse test, with unfavorable network conditions. Additional measurements show that the selected tap position affects the terminal behavior of the transformer, changing the frequency and peak value of the lower resonance point in the voltage transfer between windings.**

***Index Terms*—Transformer, black-box model, electromagnetic transients, measurements, simulation, tap setting.**

I. Introduction

TRANSIENT overvoltages are one of the root-causes of dielectric failures in transformers. The assessment of internal winding dielectric stresses is in the case of power transformers routinely performed by the manufacturers using in-house calculation programs. These programs make use of a detailed description of the transformer windings with circuit element parameters obtained using analytical expressions or Finite Element calculations, see [1] and references therein for an overview of methods. It has been shown [2] that when applied to a common geometry, the calculation programs by different manufacturers generally give similar results for the peak value of external and internal voltages when applying a lightning impulse voltage to the transformer. However, substantial differences were found for the resonance frequencies and damping. This fact raises concerns about the suitability of the manufacturer's models when applied in simulations involving general overvoltages that result from the connected system. On the other hand, measurement-based black-box models can provide quite accurate results [3]-[7] for the voltage on external terminals, although the transformer must first be built before any measurements can be performed.

One of the dielectric weak parts of a transformer is the regulating winding which, depending on the selected tap position, can exhibit strong internal resonances. In the 1970s, American Electric Power experienced several failures in auto-transformer regulating windings [8], with resonant voltage build-up as root-cause. It is therefore of interest to extend the capability of the black-box model approach to also include points in the regulating winding.

CIGRE JWG A2/C4.52 has in 2016 performed a measurement campaign on a single-phase and a three-phase transformer in order to assess/improve the accuracy of currently applied white-box models, and to provide input for black-box and grey-box modeling. The measurements involve frequency domain and time domain measurements at the transformer external terminals and at some internal points.

This paper reports results obtained for black-box-modeling of the single-phase three-winding transformer. In addition to the four external terminals, the measurements include voltage transfer from external terminals to three points in the regulating winding. From the measurements, a wide-band model is extracted which can be applied in transient simulation in an EMTP-type environment. The various steps in the measurement and modeling procedure are described with emphasis on accuracy preservation. Also, the effect of the tap changer setting on transferred overvoltages between the windings is investigated. Finally, the model is applied in a transient simulation where a resonant voltage build-up takes place in the regulating winding due to ground fault initiation in a feeding cable. The resulting overvoltages are compared with those arising in the standard lightning impulse test.

Manuscript received November 17, 2016. Revised March XXX, 2017.

B. Gustavsen is with SINTEF Energy Research, N-7465 Trondheim, Norway (e-mail: bjorn.gustavsen@sintef.no).

A. Portillo is an independent consultant in transformers, Brenda 5920, 11400, Montevideo, Uruguay (e-mail: acport18@gmail.com).

R. Rodrigo is with WEG Transformers México, km 3.5 Carretera Jorobas Tula, Huehuetoca, México (e-mail: rronchi@weg.net).

A. Mjelve is with Hafslund Nett AS, N-0247 Oslo, Norway (e-mail: asgeir.mjelve@hafslund.no).

The work was supported financially by WEG Transformers and Hafslund Nett AS. Additional support was received from ABB, Alstom/GE, EdF, CG Power, Machinenfabrik Reinhausen (MR), and SMIT Trafo.

II. Transformer Unit And Measured Quantities

The transformer is a 50 MVA single-phase three-winding transformer with rated voltages 230/69/13.8 kV at 60 Hz. The core has one mid-leg and two return legs. The internal connections are shown in Fig. 1. The regulating winding is an interleaved disk winding with 10 circuits. The online tap changer (OLTC) has 11 tap positions and the polarity of this winding is reversible, giving a total of 21 tap positions.

The measurements were performed with the transformer active part inside the tank, but without oil, lid and bushings. This paper shows results for measurements with the tap changer in mid position at position Nom+, i.e. with the moving contact "k" in Fig. 1 in position "+" and with the moving contact H0 in R11. It is observed that in this tap setting, R1 has no galvanic connection to other parts in the transformer, thereby being susceptible to voltage oscillations and therefore vulnerable to overvoltages.

The external connection points H1, H0, X1, X0, Y1 and Y2 were brought to the rim of the tank (Fig. 2) where they were made available for the measurement equipment which was placed on top of a scaffolding. The applied connection leads were those already installed for connecting H1 and X1 to the bushings as well as additional leads for bringing the remaining connection points to the rim. Three additional measurement leads were installed that allowed measurement at three internal points in the regulating winding: the two extreme ends (R1, R11) and a point (R5) near the mid-point (R6). A braided wire was clamped to the tank rim and used as ground reference in the measurements.

Using a setup similar to the one in [4], the admittance matrix was measured with respect to the four external terminals H1, X1, Y1, Y2, with terminals H0 and X0 grounded at the tank rim. In addition, two identical voltage probes were used for measuring voltage transfer functions from these four external terminals to the three points in the regulating winding, R1, R5, and R11. These points are labeled by numbers 1, 5 and 11 in Fig. 1

Tables I and II define the node labeling used in this work as well as the type of measurements that were performed.

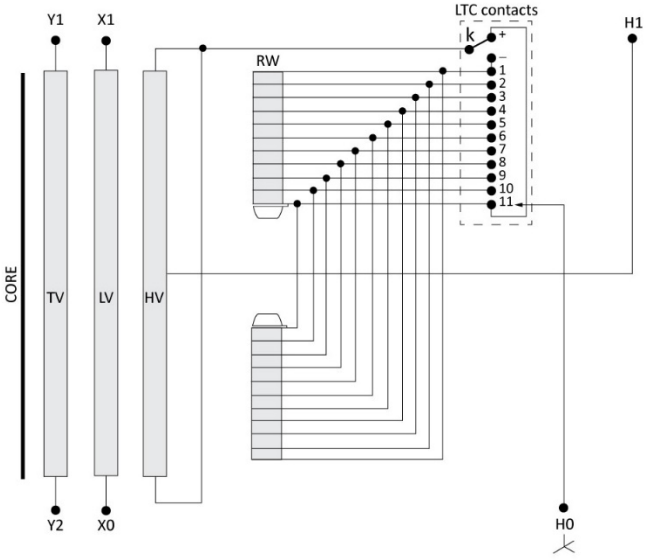

Fig. 1. Single-phase transformer with tap setting Nom+.

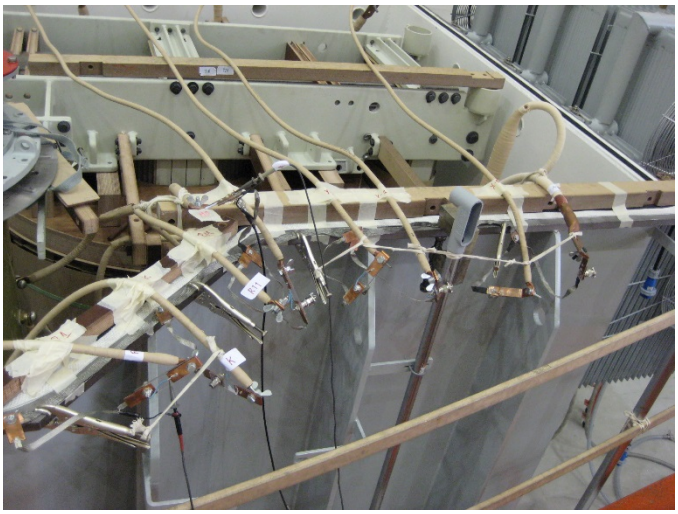

Fig. 2. Measurement connections.

Table I External Nodes (Terminals)

Node	Terminal	Description	Measurement type
1	H1	HV winding	Admittance
2	X1	LV winding	Admittance
3	Y1	Tertiary winding.	Admittance
4	Y2	Tertiary winding.	Admittance

Table II Internal Nodes

Node	Terminal	Description	Measurement type
5	R1	Tap position 1	Voltage transfer
6	R5	Tap position 5	Voltage transfer
7	R11	Tap position 11	Voltage transfer

III. Black-Box Modeling Using Combined Admittance and Voltage Transfer Modeling

A. Requirements

Since the model is to be utilized in an EMTP-type simulation program, it is essential that the model does not lead to unstable simulation results. This requirement is satisfied provided that that 1) the model to be extracted has stable poles only, and 2) the model is passive, i.e. it cannot generate power over its n terminals. Passivity entails that the model's admittance matrix $\mathbf{Y}$ is positive for all frequencies, i.e.

$$\lambda_i\{\mathbf{Y}(\omega)+\mathbf{Y}^H(\omega)\}>0,\ \ \forall\omega, i=1\ldots n \qquad (1)$$

where the operator $\lambda\{:\}$ extracts the eigenvalues of its argument.

The stable poles requirement is easily enforced with the adopted modeling approach described in Section IV. The passivity requirement (1) is much harder to achieve as it requires to perturb the model's parameters within a non-linear optimization problem. It is the experience that the difficulty with loss of passivity greatly increases with the number of terminals n to be considered in the model.

B. Approach

With this transformer, there are only four external terminals (H1, X1, Y1, Y2) that will be connected to the external system while the three internal points (R1, R5, R11) are observation

points for voltage. To reduce difficulties with passivity violations we therefore create a model having only four external terminals while the voltage on the internal points are obtained via voltage transfer function measurements for which there are no passivity requirement. The procedure is outlined below and described in detail in Sections IV and V.

The input for the modeling is a measurement of the terminal admittance matrix $\mathbf{Y}(\omega)$ with respect to the external terminals and the voltage transfer matrix $\mathbf{H}(\omega)$ from external terminals to internal points, see Fig. 3. $\mathbf{Y}$ relates the voltages and currents at the transformer external terminals (2) while $\mathbf{H}$ determines the internal voltages with the external voltages as input (3).

$$\mathbf{i}_{\text{ext}}^{4\times1}(\omega) = \mathbf{Y}^{4\times4}(\omega)\,\mathbf{v}_{\text{ext}}^{4\times1}(\omega) \tag{2}$$

$$\mathbf{v}_{\text{int}}^{3\times1}(\omega) = \mathbf{H}^{3\times4}(\omega)\,\mathbf{v}_{\text{ext}}^{4\times1}(\omega) \tag{3}$$

Matrices $\mathbf{Y}$ and $\mathbf{H}$ are to be fitted with multi-port rational functions that are expressed on state-space form,

$$\mathbf{Y}(\omega) = \mathbf{C}^{Y}(s\mathbf{I} - \mathbf{A}^{Y})^{-1}\mathbf{B}^{Y} + \mathbf{D}^{Y} \tag{4}$$

$$\mathbf{H}(\omega) \cong \mathbf{C}^{H}(s\mathbf{I} - \mathbf{A}^{H})^{-1}\mathbf{B}^{H} + \mathbf{D}^{H} \tag{5}$$

Both models are required to have stable poles only. The passivity requirement only applies to the admittance model since the voltage transfer model does not interact with the external circuit.

The two state-space models (4) and (5) are utilized in an EMTP-type time domain simulation environment as shown in Fig. 4. The admittance model is connected to the power system and the simulation gives the voltages at the transformer external terminals. These (four) voltages are used as input to the voltage transfer block whose outputs are the voltage waveforms at the (three) internal nodes.

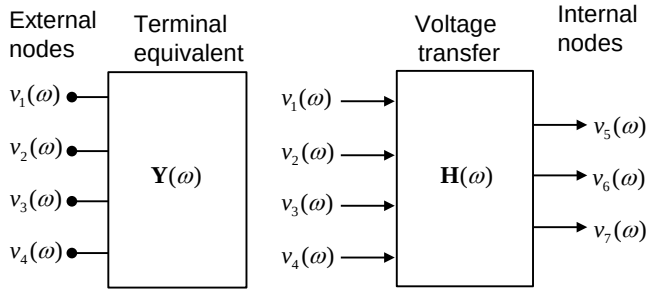

Fig. 3. External and internal nodes.

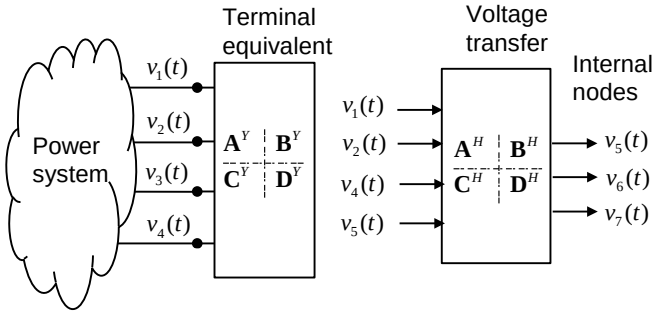

Fig. 4. Inclusion of model in time domain simulation.

IV. Admittance Modeling

A. Measurements

Fig. 5 shows the measured elements of the admittance matrix $\mathbf{Y}$ with respect to the four external terminals. It is observed that the four elements that are related to the tertiary winding (terminals 3 and 4) are practically equal in magnitude at frequencies below 10 kHz. This result is due to the tertiary winding being ungrounded which causes the common mode component, which corresponds to the capacitive charging current, to approach zero as frequency is reduced. This behavior is however inaccurately represented in the short-circuit measurement which leads to error magnifications in calculations of voltage transfers to the tertiary winding. This problem is demonstrated in Fig. 6 where the voltage transfer from terminal 2 (X1) to open terminals 1 (H1), 3 (Y1) and 4 (Y2) has been calculated from the measured $\mathbf{Y}$. It is seen that excessive errors arise at frequencies below 10 kHz. Additional errors exist at higher frequencies as well but they have a different cause which is eliminated in Section IV.B.

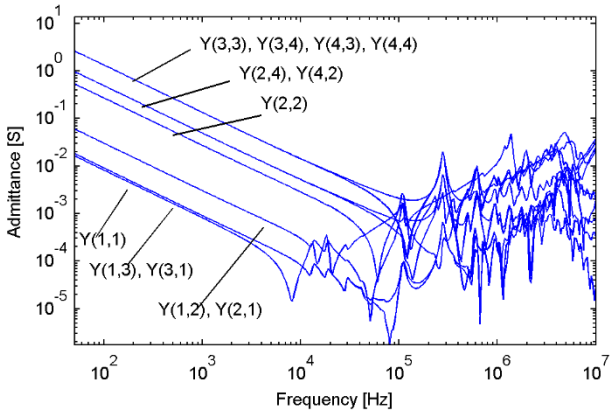

Fig. 5. Admittance matrix elements.

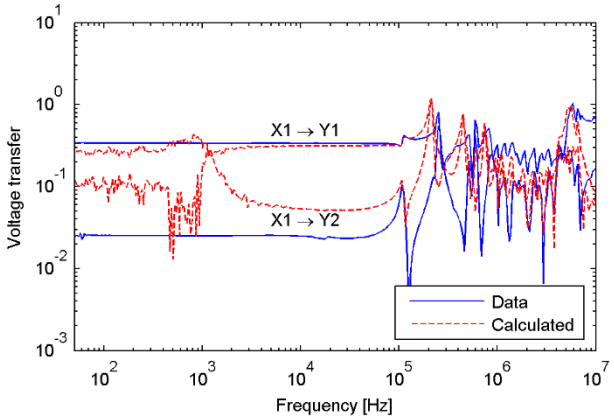

Fig. 6. Voltage transfer from X1 to Y1 and Y2, with H1 open.

In order to overcome the accuracy limitations, we will explicitly model the common mode components. Consider the matrix partitioning of $\mathbf{Y}$ in (6). As already mentioned, the 2×2 block associated with Y1 and Y2 has a very small (common mode) eigenvalue. It can be further shown that the coupling from H1 and X1 to Y1 and Y2 will also have a very small common mode component at low frequencies, which must be accurately represented.

$$\mathbf{Y} = \begin{array}{c} \begin{matrix} \text{H1} & \text{X1} & \text{Y1} & \text{Y2} \end{matrix} \\ \left[\begin{array}{c:c|cc} Y(1,1) & Y(1,2) & Y(1,3) & Y(1,4) \\ \hdashline Y(2,1) & Y(2,2) & Y(2,3) & Y(2,4) \\ \hline Y(3,1) & Y(3,2) & Y(3,3) & Y(3,4) \\ Y(4,1) & Y(4,2) & Y(4,3) & Y(4,4) \end{array}\right] \end{array} \begin{matrix} \text{H1} \\ \text{X1} \\ \text{Y1} \\ \text{Y2} \end{matrix} \qquad (6)$$

Additional measurements were performed with terminals 3 and 4 bonded, see Fig. 7. The admittance measurement of the resulting 3×3 matrix **Y**' now directly reveals the common mode component associated with Y1 and Y2.

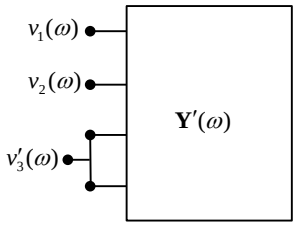

Fig. 7. Common mode admittance measurements.

Fig. 8 shows elements $Y'(3,3)$, $Y'(3,1)$ and $Y'(3,2)$. The elements at frequencies below 10 kHz are replaced with the expected capacitive behavior (straight lines) that was deduced from the 10 kHz sample point. These modified measurements were next used for replacing the common mode behavior of the original 4×4 **Y** as follows.

1. Consider the 2×2 sub-matrix (block) associated with terminals 3 and 4 which consists of elements *Y*(3,3), *Y*(3,4), *Y*(4,3), and *Y*(4,4). For this sub-matrix, subtract from each row *i* the average of the row-sum, and from each column *j* the average of the column sum. Add to all four elements the measured element $Y'(3,3)$ divided by four
2. Subtract from elements *Y*(3,1) and *Y*(4,1) the average of the two elements, and add to the two elements the measured $Y'(3,1)$ divided by two. Copy the two modified elements into position *Y*(1,3) and *Y*(1,4).
3. Subtract from elements *Y*(3,2) and *Y*(4,2) the average of the two elements, and add to the two elements the measured $Y'(3,2)$ divided by two. Copy the two modified elements into position *Y*(2,3) and *Y*(2,4).

The above replacement is only made at frequencies below 10 kHz as the accuracy was otherwise found to deteriorate at higher frequencies.

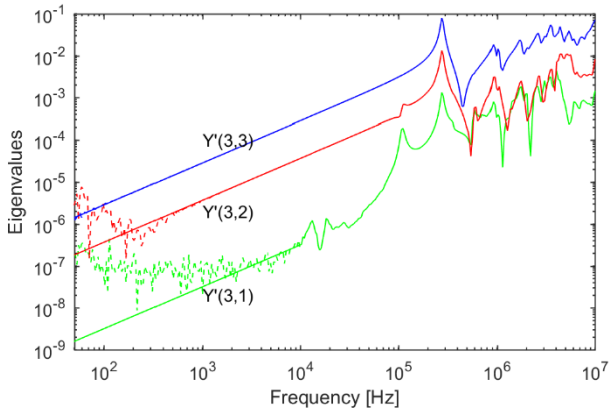

Fig. 8. Common mode measurements. Dashed lines: direct measurement; Solid lines: replacement with capacitive behavior below 10 kHz.

B. Elimination of Cable Effects

The admittance measurements were performed using coaxial cables of length 3 m. The effect of the measurement cables was removed from **Y** using the transmission line-based cable elimination method described in [10].

Fig. 9 compares the calculated voltage transfer from X1 to Y1 and Y2 (with H1 open), similarly as in Fig. 6. It is observed that the agreement with the directly measured voltage transfers are now greatly improved over the full frequency band. This result is due to 1) the special treatment of the common-mode components in Section IV-A which improves the accuracy at low frequencies, and 2) the cable elimination which improves the accuracy at high frequencies.

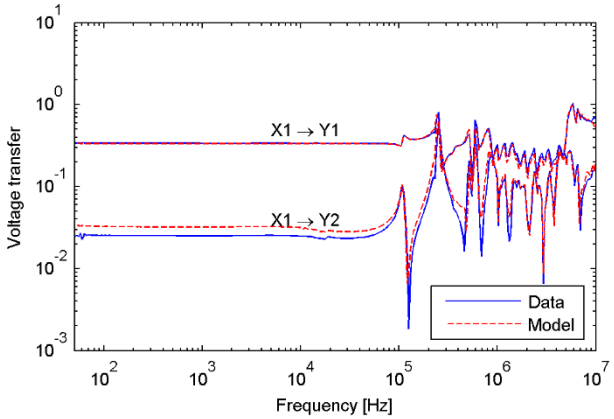

Fig. 9. Voltage transfer from X1 to Y1 and Y2 utilizing common mode measurements and elimination of cable effects.

C. Model Extraction

In order to preserve the small eigenvalues buried in **Y** during the model extraction step, we apply the method of a mode-revealing transformation [11] which makes use of a real-valued, orthogonal transformation matrix **Q**. This matrix is calculated via the eigenvector matrix **T** of **Y** at the low frequency sample where the eigenvalue ratio of **Y** is maximum. The real part of **T** is subjected to singular value decomposition

$$\mathrm{Re}\{\mathbf{T}\} = \mathbf{U}\boldsymbol{\Sigma}\mathbf{V}^H \qquad (7)$$

and replaced with its nearest orthogonal approximation,

$$\mathbf{Q} = \mathbf{U}\mathbf{V}^H \tag{8}$$

The procedure for obtaining and applying **Q** is described in detail in [11].

Q is applied as a similarity transformation (9) which achieves that that the small eigenvalues of **Y** become more visible in the transformed matrix $\tilde{\mathbf{Y}}$ while preserving the passivity properties of **Y**.

$$\tilde{\mathbf{Y}}(\omega) = \mathbf{Q}^T \mathbf{Y}(\omega)\mathbf{Q} \tag{9}$$

The transformed matrix $\tilde{\mathbf{Y}}$ is subjected to pole-residue modeling (10) [12], [13] and subsequent passivity enforcement [14]. Fig. 10 shows the elements of $\tilde{\mathbf{Y}}$ and its rational approximation using N^Y=80 pole-residue terms. It is observed that the transformed matrix has at low frequencies elements that resemble the small common-mode elements in Fig. 8.

Finally, a back-transformation (11) is applied to each residue matrix, giving the rational approximation for **Y** itself. Fig. 11 shows the final result for the rational approximation of **Y**. For use in EMTP-RV, the pole-residue model (11) is converted into a state-space model (4) as described in [9].

$$\tilde{\mathbf{Y}}(\omega) \cong \tilde{\mathbf{D}}^Y + \sum_{m=1}^{N^Y} \frac{\tilde{\mathbf{R}}_m^Y}{s - a_m^Y} \tag{10}$$

$$\mathbf{Y}(\omega) \cong \mathbf{Q}(\tilde{\mathbf{D}}^Y + \sum_{m=1}^{N^Y} \frac{\tilde{\mathbf{R}}_m^Y}{s - a_m^Y})\mathbf{Q}^T = \mathbf{D}^Y + \sum_{m=1}^{N^Y} \frac{\mathbf{R}_m^Y}{s - a_m^Y} \tag{11}$$

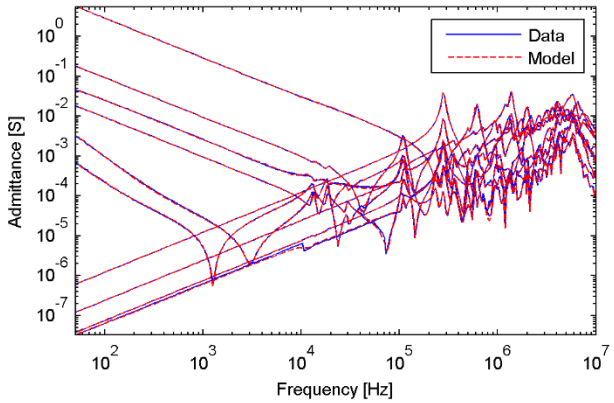

Fig. 10. Fitted elements of $\tilde{\mathbf{Y}}$.

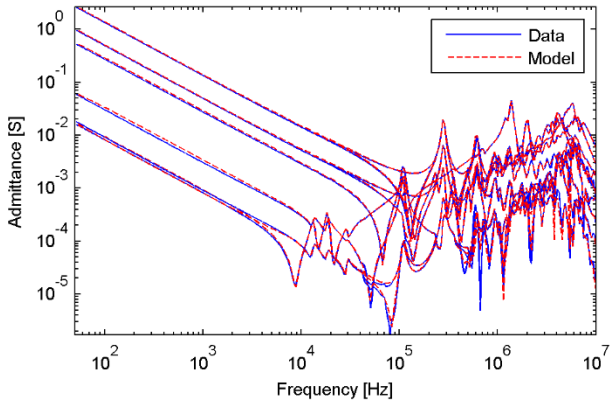

Fig. 11. Final model of **Y**.

V. Voltage Transfer Modeling

Using two identical voltage probes, the voltage transfer from external terminals 1-4 to internal nodes 5-7 were performed directly on the transformer terminals without the use of coaxial cables. The measurements define the voltage transfer by (3) where the four columns of **H** are subjected to rational fitting by a common pole set of N^H=100 poles (12). The pole-residue models are converted [9] into state-space models which are concatenated into a single model (5).

$$\mathbf{h}_i(\omega) \cong \mathbf{r}_{0,i} + \sum_{m=1}^{N^H} \frac{\mathbf{r}_{i,m}}{j\omega - a_{i,m}} \tag{12}$$

Fig. 12 shows the measured elements along with their rational approximation. It is observed that strong resonances appear in R1 and R5 at around 18 kHz and 1 MHz.

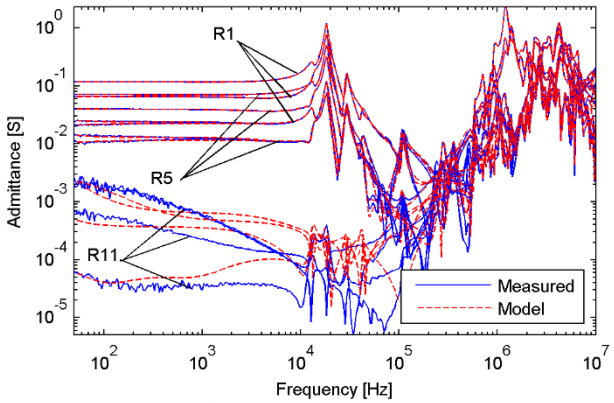

Fig. 12. Rational model of **H** (N=100 poles per column).

VI. Time Domain Validation

A. Convolution-Based Approach

The final validation of a model should be performed in the time domain since seemingly small model errors in the frequency domain can lead to large errors in the time domain as the simulation time progresses. In this work, we used a slightly different approach based on direct voltage transfer function measurements in the frequency domain with terminal conditions that correspond to the test condition of the accuracy assessment. The transfer functions are measured one-by-one on the terminals using two identical voltage probes. The voltage transfer functions are fitted with a high-order rational function, allowing time domain simulation via recursive convolution [15]. The approach is accurate since there are no matrix manipulations involved. Compared to a direct time domain measurement, it has the advantage that the response can be calculated for any input wave shape. In the following subsections these convolution-based simulations are denoted as "Measured" although they have been derived from frequency domain data.

B. Voltage Application on H1

In this test, the voltage is applied to terminal H1 with H0 and X0 grounded and with X1, Y1 and Y2 open. The voltage

transfers from terminal H1 to X1, Y1, Y2, R1, R5 and R11 are measured and fitted with rational functions.

Fig. 13 shows the voltage responses on the external terminals as obtained by the admittance model (2) when applying a 1 Volt lightning impulse wave on H1. The agreement is excellent with only a small difference in the oscillation frequency.

Fig. 14 shows the simulated voltage on R1, R5, and R11 as obtained with the voltage transfer model (3) which has the simulated waveforms in Fig. 13 as input. A zoomed view is provided in Fig. 15. Again, a very accurate result has been obtained. Similar accuracy was obtained when applying the voltage excitation on the low-voltage side (X1).

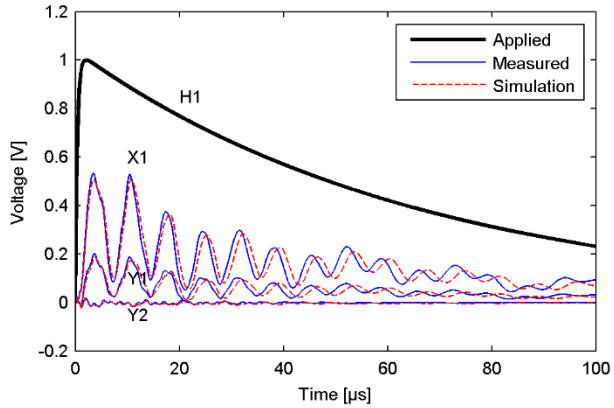

Fig. 13. Voltage response on external nodes.

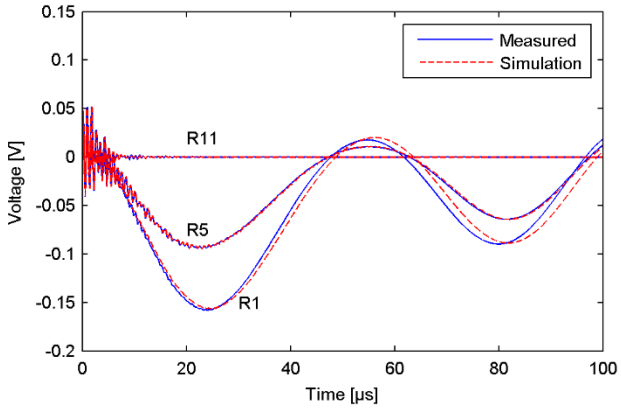

Fig. 14. Voltage response on internal nodes.

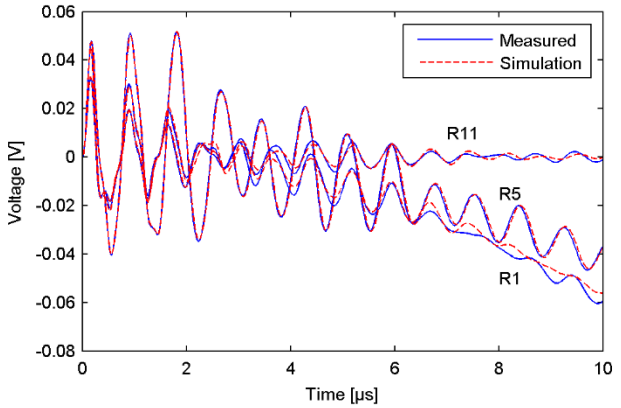

Fig. 15. Voltage response on internal terminals (zoomed view).

VII. Impact of Tap Setting on Terminal Behavior

The selected tap setting will impact the overvoltages that occur in the regulating winding. In addition, the tap setting also affects the transferred overvoltages between the windings. The transferred voltage was investigated by measuring the admittance matrix with respect to terminals H1 and X1 with the tertiary terminals (Y1, Y2) open. The elements of the associated 2×2 admittance matrix are shown in Fig. 16, with nodes 1 and 2 denoting H1 and X1, respectively. The elements are shown for the transformer tap setting in position Max, Nom+, Nom- and Min. It can be seen that a noticeable difference exists between the tap positions at frequencies below 30 kHz. The difference between the two mid-positions Nom+ and Nom- is however very small. Above 30 kHz, the differences between all curves are small until 1 MHz where noticeable differences can again be observed.

From the admittance matrices, the voltage transfer function X1 to H1 was calculated, see Fig. 17. It can be observed that the tap setting greatly affects the first resonance peak at about 7 kHz. The peak is substantially reduced and shifted towards higher frequencies as the tap position is moved from Max to Mid (Nom+/Nom-) and Min. These results imply that a general black-box model should be created for more than a single tap position to properly represent the low frequency resonance. The change to the low frequency resonance is quantified in Table III.

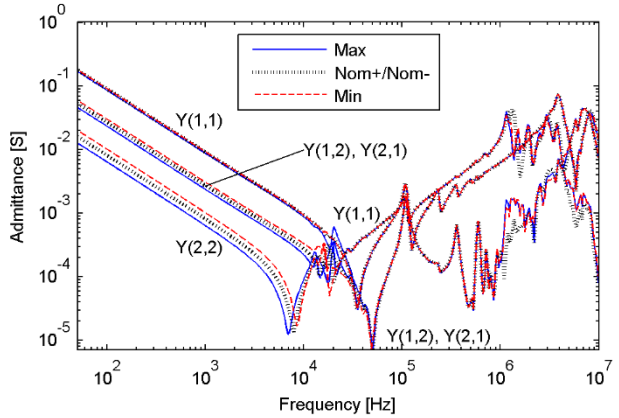

Fig. 16. Measured terminal admittance with respect to H1 and X1, with tertiary terminals (Y1, Y2) open. Impact of tap setting.

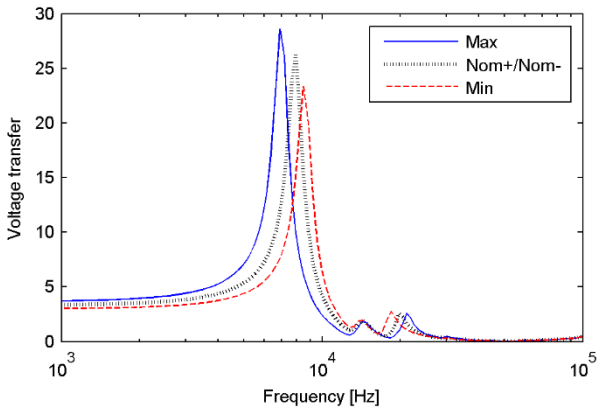

Fig. 17. Calculated voltage transfer from X1 to H1.

TABLE III LOW-FREQUENCY RESONANCE IN VOLTAGE TRANSFER FROM X1 TO H1

Position	f_0 [kHz]	$\|H_0\|$
Max	6.9	29
Mid	7.9	26
Min	8.5	23

VIII. OVERVOLTAGES CAUSED BY GROUND FAULT INITIATION

We return to the complete transformer model in tap Nom+ and demonstrate its potential application in a transient simulation study. Three transformer units are connected into a three-phase bank as shown in Fig. 18 by connecting the tertiary windings into delta. The transformer is fed from a substation via a cable as shown in Fig. 19. The cable is modeled as three lossless single-phase lines with propagation characteristics as shown in Table IV, and with mutual coupling between phases neglected. The system overhead lines (OHL) are single-circuit three-phase lines over a lossy earth with resistivity 100 Ω·m. The conductor data are given in Table V by position (x, y) diameter (d) and DC resistance (R_{dc}). The overhead lines are modeled in EMTP-RV as frequency-dependent multi-conductor lines.

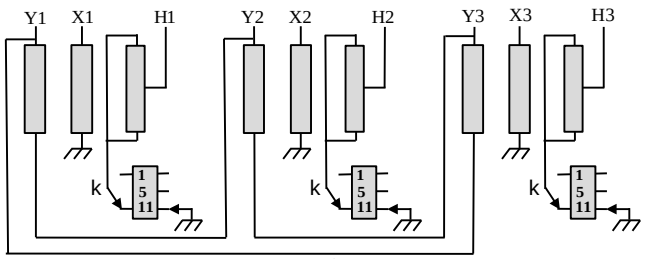

Fig. 18. Connecting three 1-phase transformers into a 3-phase bank.

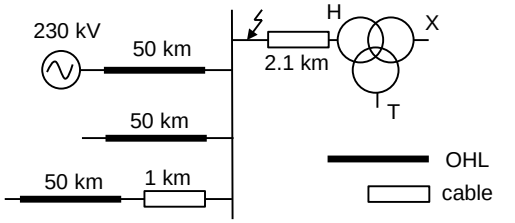

Fig. 19. Ground fault initiation in phase 1 of transformer feeding cable.

TABLE IV CABLE PROPAGATION PARAMETERS

Characteristic impedance, Z_C	Velocity, v
30 Ω	160 m/μs

TABLE V OVERHEAD LINE CONDUCTOR PARAMETERS

Conductor no.	1	2	3	4	5
x [m]	−7.6	0	7.6	−5	5
y [m]	19.5	19.5	19.5	24.4	24.4
d [cm]	3.51	3.51	3.51	1.94	1.94
R_{dc} [Ω/km]	0.045	0.045	0.045	0.151	0.151

An ideal ground fault occurs in phase 1 in the substation at voltage maximum, which is represented in the simulation by a closing switch. The ground fault initiation results in a voltage oscillation in phase 1 on the transformer HV side. The dominant frequency component results from quarter-wave oscillation in the line stub and is estimated by (13) to be 19 kHz with l=2.1 km and v=160 m/μs. This oscillation frequency coincides with the resonance peak in voltage transfer from the HV terminal to the internal points in Fig. 12.

$$f_{\lambda/4} = \frac{v}{4l} \tag{13}$$

Fig. 20 shows the simulated voltage waveforms on the transformer external terminal H1 and at the internal points (R1, R5, R11), in the faulted phase. It is observed that the internal voltages undergo a resonant build-up, giving a peak value of about 200 kV. For comparison, the ditto peak voltage during the lightning impulse test (all terminals grounded except H1) with U_{BIL}=1050 kV peak voltage was found to reach only 182 kV. Usage of internal surge arresters should therefore be considered in order to control the overvoltages.

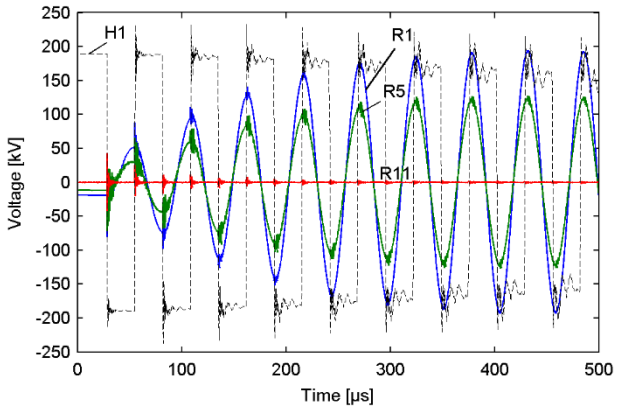

Fig. 20. Voltage on external terminals and internal points in phase 1.

The damping of the impinging voltage on the HV terminal is greatly increased when replacing the cable with an overhead line due to its higher characteristic impedance. To see this, the 2.1 km cable between the bus and the transformer is replaced with a 4 km overhead line. The quarter-wave resonance frequency of the OHL is the same as for the 2.1 km overhead line, i.e. 19 kHz. The overvoltage in R1 in relation to the peak value of the 60 Hz stationary voltage is listed in Table VI when the transformer feeding line is either a cable (Fig. 21) or an OHL. The lower overvoltage in the OHL case is due to its lower characteristic impedance, and due to mutual coupling between the phase conductors.

TABLE VI OVERVOLTAGE IN R1 FROM GROUND FAULT INITIATION

Feeding line	Overvoltage factor in R1
Underground cable (2.1 km)	10.2
Overhead line (4 km)	4.4

IX. RESONANT OVERVOLTAGE CONDITIONS

The simulation example in Section VIII focused on an example with ground fault initiation on the far end of a feeding cable on the transformer high-voltage side. The cable length was such that cable voltage oscillating frequency on the transformer side matched an internal resonance of the transformer, and the duration of the oscillation was sufficient for the voltage in the regulating winding to reach nearly its maximum value. Reference [16] discusses conditions and situations where oscillating overvoltages can result on the

transformer terminals and thus start an initial resonant voltage buildup inside the transformer. It is shown that capacitor bank energization can lead to similar overvoltages as ground fault initiation when the capacitor bank is directly connected to the bus at the cable far end side. Cable energization involving two cables of equal length can lead to overvoltages of about half the peak value as in the ground fault case. Energizing a (short) feeding cable from a substation where many other (long) cables are connected will also lead to an oscillating voltage on the transformer terminals, but the duration of the oscillation is often not sufficient for the voltage buildup inside the transformer to reach high voltage levels.

X. Discussion

A. Effect of Oil and Bushings

The measurements were performed with the transformer in tank, but without oil. Measurements in oil are possible but such approach is less attractive for reasons related to time consumption and cost. The impact of the missing oil is that the partial capacitances between transformer internal parts is too low, which is affects both admittance and voltage transfer functions. In general, reducing the capacitances will shift resonances towards high frequencies. This impact of the missing oil should be clarified by further studies. The measurements were further performed without presence of the bushings. The bushings can however be represented by lumped shunt capacitances that can be added to the model.

B. Advantages of Voltage Transfer Measurements

It was already explained in Section III.A that the use of voltage transfer measurements to internal points offers advantages regarding model passivity, compared to an approach which treats these points as external terminals in an admittance measurement. There are other advantages as well. With a pure admittance approach, the calculation of the three internal voltages effectively involves inversion of a 3×3 submatrix of the 7×7 $\mathbf{Y}$. It is the experience that such inversion can lead to substantial error magnifications of measurement errors and fitting errors alike.

C. Practical Limitations

The proposed approach is not a substitute for a white-box model as it is can only provide information about the voltage on (a few) internal points that are accessible from the outside, in this case points in the tap changer. The attractiveness of the approach is the high accuracy that can be achieved. In the case of failure investigations, the proposed approach seems very useful as one can then sometimes perform invasive measurements on the outer winding parts.

D. Industrial Application

The application of the approach is at present limited to specialists since it requires some customized equipment and non-standard calculation programs. Still, the approach could be adopted by the manufacturers and consultants. The most challenging part of the procedure is the admittance measurement which is needed for obtaining the model used for simulating the voltage on external terminals. But several modifications could be made. For instance, a simplified model could be used for obtaining the voltage at the transformer external terminals, e.g. a 50/60 Hz model with lumped capacitances. That way, the need for admittance measurements is avoided and the voltage to open terminals (including internal points) can be obtained by voltage transfer measurements alone. The voltage transfer measurements are easy to perform and generally leads to quite accurate results as error magnification is not an issue.

E. Application to Other Winding Configurations

In the presented approach we used a model obtained from admittance measurements for simulating the voltage on the external terminals. Admittance measurements can be difficult to achieve with sufficient accuracy if the transformer has ungrounded windings. In the past it was shown how to handle this situation for a two-winding three-phase transformer with one ungrounded winding [17] by introducing zero-sequence measurements. In the present work, we achieved in a similar way accurate measurements of a three-winding single-phase transformer having one ungrounded winding, by introducing common-mode measurements. If a transformer has two ungrounded windings, the procedure for admittance measurements must be further modified.

XI. Conclusion

This work has demonstrated that overvoltages in the regulating winding can be simulated using a black-box model approach which combines an admittance-based terminal equivalent with a voltage transfer model. The approach offers excellent accuracy and compatibility with EMTP-type simulation programs.

The presence of an ungrounded tertiary winding in the given transformer causes error magnifications at lower frequencies. This problem is overcome by explicitly representing the common mode components during measurement and model extraction.

Usage of the model in a transient simulation study shows that internal voltages in the regulating winding can in resonant conditions exceed the voltage that occurs in the lightning impulse test. The modeling approach can therefore be a valuable tool for identifying network conditions where such resonant voltage buildup is likely to occur.

The tap setting can substantially impact the terminal admittance matrix below 10 kHz, thereby impacting the lower-frequency resonance frequencies. Black-box terminal models should therefore be provided for several tap settings, e.g. Min. Mid and Max positions.

XII. Acknowledgment

The authors thank their colleagues in CIGRE JWG A2/C4.52 for their support and many useful discussions.

XIII. References

[1] R.M. Del Vecchio, B. Poulin, P.T. Feghali, D.M. Shah, and R. Ahuja, *Transformer design principles*, CRC Press, 2010.

[2] CIGRE Technical Brochure 577A, "Electrical transient interaction between transformers and the power system. Part 1 – Expertise", CIGRE JWG A2/C4.39, April 2014.

[3] A. Morched, L. Marti, and J. Ottevangers, "A high frequency transformer model for the EMTP," *IEEE Trans. Power Delivery*, vol. 8, no. 3, pp. 1615-1626, July 1993.

[4] B. Gustavsen, "Wide band modeling of power transformers", *IEEE Trans. Power Delivery*, vol. 19, no. 1, pp. 414-422, Jan. 2004.

[5] A. Borghetti, A. Morched, F. Napolitano, C.A. Nucci, and M. Paolone, "Lightning-induced overvoltages transferred through distribution power transformers", *IEEE Trans. Power Delivery*, vol. 24, no. 1, pp. 360-372, Jan 2009.

[6] Filipovic-Grcic, B. Filipovic-Grcic, I. Uglesic, "High-frequency model for the power transformer based on frequency-response measurements", *IEEE Trans. Power Delivery*, vol. 30, no. 1, pp. 34-42, Feb. 2015.

[7] B. Gustavsen and B. Tandstad, "Wide band modeling of a 45-MVA generator step-up transformer for network interaction studies", *Electric Power Systems Research*, vol. 142, pp. 47-57, Jan. 2017.

[8] H.B. Margolis, J.D.M. Phelps, A.A. Carlomagno, and A.J. McElroy, "Experience with part-winding resonamce in EHV auto-transformers: Diagnosis and corrective measures", *IEEE Trans. Power Apparatus and Systems*, vol. 94, no. 4, pp. 1294-1300, July/August 1975

[9] B. Gustavsen, "Computer code for rational approximation of frequency dependent admittance matrices", *IEEE Trans. Power Delivery*, vol. 17, no. 4, pp. 1093-1098, October 2002.

[10] B. Gustavsen, "Eliminating measurement cable effects from transformer admittance measurements", *IEEE Trans. Power Delivery*, vol. 31, no. 4, pp. 1609-1617, August 2016.

[11] B. Gustavsen, "Rational modeling of multi-port systems via a symmetry and passivity preserving mode-revealing transformation", *IEEE Trans. Power Delivery*, vol. 29, no. 1, pp.199-205, February 2014.

[12] B. Gustavsen and A. Semlyen, "Rational approximation of frequency domain responses by vector fitting", *IEEE Trans. Power Delivery*, vol. 14, no. 3, pp. 1052-1061, July 1999.

[13] D. Deschrijver, M. Mrozowski, T. Dhaene, and D. De Zutter, "Macromodeling of multiport systems using a fast implementation of the vector fitting method", *IEEE Microwave and Wireless Components Letters*, vol. 18, no. 6, pp. 383-385, June 2008.

[14] B. Gustavsen, "Fast passivity enforcement for pole-residue models by perturbation of residue matrix eigenvalues", *IEEE Trans. Power Delivery*, vol. 23, no. 4, pp. 2278-2285, October 2008.

[15] A. Semlyen and A. Dabuleanu, "Fast and accurate switching transient calculations on transmission lines with ground return using recursive convolutions", *IEEE Trans. Power Apparatus and Systems*, vol. 94, pp. 561-575, March/April 1975.

[16] B. Gustavsen, "Study of transformer resonant overvoltages caused by cable-transformer high-frequency interaction", *IEEE Trans. Power Delivery*, vol. 25, no. 2, pp. 770-779, April 2010.

[17] B. Gustavsen, "Frequency-dependent modeling of power transformers with ungrounded windings", *IEEE Trans. Power Delivery*, vol. 19, no. 3, pp. 1328-1334, July 2004.

XIV. Biographies

Bjørn Gustavsen (M'94–SM'2003–F'2014) was born in Norway in 1965. He received the M.Sc. degree and the Dr.Ing. degree in Electrical Engineering from the Norwegian Institute of Technology (NTH) in Trondheim, Norway, in 1989 and 1993, respectively. Since 1994 he has been working at SINTEF Energy Research where he is currently a Chief Research Scientist. His interests include simulation of electromagnetic transients and modeling of frequency dependent effects. He spent 1996 as a Visiting Researcher at the University of Toronto, Canada, and the summer of 1998 at the Manitoba HVDC Research Centre, Winnipeg, Canada. He was a Marie Curie Fellow at the University of Stuttgart, Germany, August 2001–August 2002. He is convener of CIGRE JWG A2/C4.52 "High-frequency transformer and reactor models for network studies".

Álvaro Portillo (M'84–SM'2001) was born in Uruguay in 1954. He graduated in Electrical Engineering in the Uruguayan Republic University in 1979. He worked in the Uruguayan electrical utility (UTE) up to 1985 in activities related with acceptance, installation and maintenance of power transformers. From 1985 to 1999 he worked in MAK S.A. (Uruguayan manufacturer of transformers), from 2000 to 2007 as consultant in TRAFO (Brazilian manufacturer of transformers) and from 2007 up today as consultant, in developing software tools for transformers design, at WEG (Brazilian manufacturer of transformers). He is a professor at the Uruguayan Republic University since 1977, now responsible for post-graduation courses about transformers (specification, design, design review, operation, maintenance, repairs, etc.). He is member of CIGRE Transformers Study Committee and a task force leader within CIGRE JWG A2/C4.52 "High-frequency transformer and reactor models for network studies".

Rodrigo Ronchi was born in Brazil in 1980. He graduated with P.E. degree in Electrical Engineering in Fundacao Universidade Regional de Blumenau - FURB in 2008 and 2010, respectively. He worked at ABB in Blumenau up to 2005 in Engineering Department with distribution transformer design. Since 2005 he has been working at WEG Transformadores (Brazil and México) with power transformer design. He is member of CIGRE JWG A2/C4.52 "High-frequency transformer and reactor models for network studies".

Asgeir Mjelve was born in Oslo, Norway, in 1959. He received the B.Sc. degree in electrical engineering from Østfold University College, Norway, in 1980. Since 1982, he has been with Hafslund Nett, the electricity utility for the city of Oslo and surrounding areas and the largest distribution grid company in Norway. He has been working primarily with issues related to planning, design, and maintenance of substations and is also responsible for the R&D activities in Hafslund Nett. He is member of CIGRE Transformers Study Committee.